Electron wave-packet dynamics in a relativistic electromagnetic field: 3-D analytical approximation

J. Peatross*, C. Müller, and C. H. Keitel

Max Planck Institut für Kernphysik, Saupfercheckweg 1, D-69117 Heidelberg, Germany
**Permanent Address: Dept. of Physics and Astronomy, Brigham Young University, Provo, UT 84602*
peat@byu.edu

Abstract: A solution to the Klein Gordon equation for a laser-driven electron is constructed from a superposition of Volkov states. The time- and space-dependent three-dimensional superposition integral can be evaluated analytically for an initial Gaussian momentum distribution when the expression for relativistic energy is expanded in a Taylor series over the scaled initial momenta. The solution preserves many complicated wave-packet dynamics in a strong field, including so-called wave-packet shearing and the formation of multiple peaks when the wave packet spreads to the scale of the driving-field wavelength. The range of applicability of the solution applies to much of the parameter space accessible by current intense ultra-short laser systems.

OCIS codes: (270.6620) Strong-field processes; (000.1600) Classical and quantum physics.

References and links

1. G. R. Mocken and C. H. Keitel, "Quantum Signatures in Laser-Driven Relativistic Multiple Scattering," Phys. Rev. Lett. **91**, 173202 (2003).
2. G. R. Mocken and C. H. Keitel, "Quantum Dynamics of Relativistic Electrons," J. Comput. Phys. **199,** 558-588 (2004).
3. M. W. Walser, D. J. Urbach, K. Z. Hatsagortsyan, S. X. Hu, and C. H. Keitel, "Spin and radiation in intense laser fields," Phys. Rev. A **65**, 043410 (2002).
4. P. Panek, J. Z. Kaminski, and F. Ehlotzky, "Laser-Induced Compton Scattering at Relativistically High Radiation Powers," Phys. Rev. A **65,** 022712 (2002).
5. D. M. Volkov, Z. Phys. **94**, 250 (1935).
6. J. S. Román, L. Roso, and H. R. Reiss, "Evolution of a Relativistic Wavepacket Describing a Free Electron in a Very Intense Laser Field," J. Phys. B: At. Mol. Opt. Phys. **33,** 1869-1880 (2000).
7. J. S. Román, L. Plaja, and L. Roso, "Relativistic quantum dynamics of a localized Dirac Electron Driven by an Intense-Laser-Field Pulse," Phys. Rev. A **64,** 063402 (2001).
8. M. Verschl and C. H. Keitel, "Analytical Approach to Wave-Packet Dynamics of Laser-Driven Particles beyond the Dipole Approximation," Laser Phys. **15,** 529-535 (2005).
9. Y. I. Salamin, S. X. Hu, K. Z. Hatsagortsyan, and C. H. Keitel, "Relativsitic High-Power Laser-Matter Interactions," Phys. Rep. **427**, 41-155 (2006).
10. J. H. Eberly, "Interaction of Very Intense Light with Free Electrons," Progress in Optics **7**, 361-414 (1969).
11. W. Greiner, *Relativistic Quantum Mechanics: Wave Equations*, 3rd ed., Springer, Berlin (2000).
12. J.D. Bjorken and S.D. Drell, *Relativistic Quantum Mechanics* (McGraw-Hill, New York, 1964).

1. Introduction

Wave-packet dynamics for charged particles in relativistic electromagnetic fields have been investigated numerically using either the Dirac or the Klein-Gordon equation. Mocken *et al.* have performed a series of *ab initio* calculations in 2-D of electron wave-packet dynamics in strong laser fields [1,2]. The Dirac equation is needed if one wants to

#79490 - $15.00 USD Received 29 Jan 2007; revised 28 Mar 2007; accepted 1 Apr 2007; published 2 May 2007

account for spin effects. At currently available laser intensities, however, spin effects for a free electron are in most cases of little consequence, and the Klein-Gordon equation approximates well the behavior of a Dirac particle such as an electron [1,3,4]. Nevertheless, *ab initio* calculations for either equation is numerically challenging and time consuming [2].

A wave packet for a free charged particle can be constructed from a superposition of Volkov states [5], which are available as exact solutions to both the Dirac and the Klein-Gordon equation in an electromagnetic plane-wave field. That is, the applied field can have an arbitrary temporal profile but must propagate uni-directionally. Román *et al.* used this approach to explore wave-packet dynamics in a relativistic regime [6,7]. Their technique had a side effect of populating the wave function with a small amount positronic amplitude, in addition to the electron amplitude. Although the superposition integral for wave-packet construction is less numerically intensive than *ab initio* calculations, it is still challenging, especially in three dimensions, since the integration must be repeated at every point in space and time where one wishes to view the dynamics.

Volkov solutions are also available for the Schrödinger equation in an oscillating electric field, but they exist only in the dipole approximation. They do not countenance, for example, the Lorenz drift, which arises from the action of the magnetic field component. Verschl *et al.* showed how to inject this property within the framework of the Schrödinger equation for dynamics beyond the dipole approximation [8]. However, the complex dynamics that occur when a wave packet spreads to the scale of a laser wavelength (i.e. different parts of the wave packet responding to varied phase in the propagating electromagnetic field) were included only to first order.

In this article, we develop a closed analytical approximate solution to the Klein Gordon equation for a free charged particle in a strong plane-wave electromagnetic field. The three-dimensional expression, which assumes an initial Gaussian distribution in momentum, is valid well into the relativistic regime, which includes intensity parameters typical of current state-of-the-art high-intensity laser technology. We also sketch how to extend our approach to include spin effects, using the Dirac equation. The results presented in this article represent a unique and useful tool for studying wave-packet dynamics in a strong laser field. We illustrate the use of our approach through a series of computer animations, generated with very little computational overhead.

2. Volkov-state solution to Klein-Gordon equation

The Klein Gordon equation [10-12] for a spinless electron of charge $-e$ is

$$-\hbar^2 \frac{\partial^2 \Psi}{\partial t^2} = m^2 c^4 \Psi + c^2 \left(-i\hbar\nabla + e\vec{A}\right)^2 \Psi \,, \tag{1}$$

where in the radiation gauge an electromagnetic field is described solely by the vector potential $\vec{A}(z-ct)$, here taken to propagate in the z-direction with arbitrary temporal profile; $\vec{A}$ has only x and y components. Under these conditions, the Volkov states form a complete basis for a solution:

$$\Psi_{\vec{p}}^{V}(\vec{r},t) = \sqrt{\frac{mc^2}{(2\pi\hbar)^3 E}} \exp\left\{ i\frac{(\vec{p}\cdot\vec{r} - Et)}{\hbar} - \frac{i}{\hbar(p_z - E/c)} \int_{-\infty}^{z-ct} \left[e\vec{p}\cdot\vec{A}(\ell) + e^2 A^2(\ell)/2 \right] d\ell \right\}. \tag{2}$$

The energy and momentum are connected through

$$E^2 = p^2 c^2 + m^2 c^4 \,. \tag{3}$$

#79490 - $15.00 USD Received 29 Jan 2007; revised 28 Mar 2007; accepted 1 Apr 2007; published 2 May 2007

The normalization and orthogonality [10] of the Volkov states is expressed through the relativistically invariant inner-product between states with momenta $\vec{p}_1$ and $\vec{p}_2$:

$$\left\langle \vec{p}_1 \middle| \vec{p}_2 \right\rangle = \frac{i\hbar}{2mc^2} \iiint_{\text{All space}} d^3r \left[\Psi^{V*}_{\vec{p}_1}(\vec{r},t) \frac{\partial \Psi^{V}_{\vec{p}_2}(\vec{r},t)}{\partial t} - \Psi^{V}_{\vec{p}_2}(\vec{r},t) \frac{\partial \Psi^{V*}_{\vec{p}_1}(\vec{r},t)}{\partial t} \right] = \delta\left(\vec{p}_2 - \vec{p}_1\right). \quad (4)$$

We construct a wave packet from the Volkov states as follows:

$$\Psi(\vec{r},t) = \iiint_{\text{All momenta}} d^3p a(\vec{p}) \Psi^{V}_{\vec{p}}(\vec{r},t). \quad (5)$$

We choose a Gaussian superposition of states according to

$$a(p) = \frac{1}{\left(p_o\sqrt{\pi}\right)^{3/2}} \exp\left\{ -\frac{p^2}{2p_o^2} \right\}, \quad (6)$$

for which the inner product $\langle \Psi | \Psi \rangle = 1$, and the width of the momentum distribution is governed by the parameter p_o. The form of Eq. (6) dictates a frame of reference wherein the center of the wave packet is stationary in the absence of an applied field. The evolution of the wave packet is managed entirely by Eq. (5). However, since the variables $\vec{r}$ and t are entangled with the variable of integration $\vec{p}$, the three-dimensional integral must be repeated for each point in space and time in order to retrieve the wave-packet dynamics.

3. Approximations

To make progress on the integral in Eq. (5), we make a multi-variable Taylor-series expansion on Eq. (3):

$$E \cong mc^2 \left[1 + \frac{p_x^2 + p_y^2 + p_z^2}{2m^2c^2} + O\left(\frac{p^4}{m^4c^4} \right) \right]. \quad (7)$$

The momentum is restricted by the Gaussian profile in Eq. (6) to the scale of p_o. Since p_o describes the rate of wave-packet spreading only, as opposed linear motion, one expects values for p_o that lie well below mc. Note that $p_o \sim mc$ would dictate an electron wave packet confined initially to the unusually small spatial scale of a Compton wavelength. For $p_o << mc$, we may safely approximate the factor mc^2/E out in front of Eq. (2) by unity. However, we retain the quadratic terms in Eq. (7) for the first occurrence of E in the exponent of Eq. (2). For the second occurrence of E in the exponent, we utilize the following Taylor-series expansion:

$$\frac{1}{E - cp_z} \cong \frac{1}{mc^2} \left[1 + \frac{p_z}{mc} - \frac{p_x^2 + p_y^2 - p_z^2}{2m^2c^2} - \frac{p_x^2 p_z + p_y^2 p_z}{m^3c^3} + O\left(\frac{p^4}{m^4c^4} \right) \right]. \quad (8)$$

We retain only two terms of Eq. (8) when multiplying the integral of $\vec{A}$ in Eq. (2), but we retain the other terms in Eq. (8) in connection with the integral of A^2, which for high fields dominates after appreciable time.

With these approximations, Eq. (5) remains valid as long as the following conditions hold:

#79490 - $15.00 USD Received 29 Jan 2007; revised 28 Mar 2007; accepted 1 Apr 2007; published 2 May 2007

$$p_o'^4 k_C c|t| << 1\,;\; p_o'^3 |f_x|,\; p_o'^3 |f_y| << 1\,;\; p_o'^4 |f| << 1\,, \tag{9}$$

where we have introduced the definitions

$$p_o' \equiv p_o/mc\,,\quad k_C \equiv mc/\hbar\,,\quad f_x \equiv \frac{e}{\hbar}\int_{-\infty}^{z-ct} A_x d\ell\,,\quad f_y \equiv \frac{e}{\hbar}\int_{-\infty}^{z-ct} A_y d\ell\,,\text{ and }\quad f \equiv \frac{e^2}{2\hbar mc}\int_{-\infty}^{z-ct} A^2 d\ell\,. \tag{10}$$

It is clear that the last condition in Eq. (9) cannot hold at arbitrary space-time points (in particular, in the case of a continuous laser field) as the integrand is non-negative everywhere. Therefore, it is implicitly understood that the analysis is restricted to the 'region of interest' where the electron wave packet is actually present. In a continuous field, the conditions for validity can be expressed in terms of the number of applied laser cycles N. Eq. (9) then becomes $Np_o'^4 << \varepsilon$, $p_o'^3 A_o' << \varepsilon$, and $NA_o'^2 p_o'^4 << \varepsilon$, where $\varepsilon \equiv \hbar\omega / mc^2$ is the scaled photon energy and $A_o' \equiv eA_o / mc$ is the scaled vector potential.

The conditions in Eq. (9) are met over a surprisingly broad range of parameters, including for relativisitic intensities of the applied field. This is especially true if the initial momentum spread is narrow. For example, if $p_o = 10^{-3} mc$, the middle condition isn't violated until the intensity exceeds 10^{23} W/cm^2, for 800 nm light. For this wavelength and intensity, the final condition of Eq. (9) holds for several tens of laser cycles, and the first condition holds for more than 10^5 laser cycles. As the initial momentum spread of the wave packet increases, the maximum tolerated applied intensity drops quickly. These restrictions are discussed further in connection with examples given in section 5.

4. Evaluation

Under the preceding approximations, the integrals for p_x and p_y disentangle from each other with exponents containing only linear and quadratic terms in p_x and p_y. The two integrals can be performed analytically, and the resulting expression for $\Psi(\vec{r},t)$ becomes

$$\Psi(\vec{r},t) = \left(\frac{k_C p_o'}{\sqrt{\pi}}\right)^{3/2} \frac{e^{-i\eta_t^-}}{\sqrt{2\pi}} \int_{-\infty}^{\infty} d\zeta e^{-\frac{1}{2}\left(1+ip_o'^2\eta_t^-\right)\zeta^2 + ip_o'\eta_z\zeta} \frac{e^{-p_o'^2 \frac{\eta_x^2+\eta_y^2+2p_o'\left(f_x\eta_x+f_y\eta_y\right)\zeta+p_o'^2\left(f_x^2+f_y^2\right)\zeta^2}{2\alpha\left[1+i2p_o'^3\frac{f}{\alpha}\zeta\right]}}}{\alpha\left[1+i2p_o'^3\frac{f}{\alpha}\zeta\right]}, \tag{11}$$

where $\alpha \equiv 1 + ip_o'^2\eta_t^+$, $\eta_t^\pm \equiv k_C ct \pm f$, $\eta_x \equiv k_C x + f_x$, $\eta_y \equiv k_C y + f_y$, and $\eta_z \equiv k_C z + f$.

To perform the remaining integral (over the dimensionless variable $\zeta \equiv p_z/p_o$, which is on the order of unity), we must make further approximations. Fortunately, this can often be done while remaining within the purview of the approximations made in Eq. (9). In the exponent, we expand the following factor:

$$\frac{1}{1+i2p_o'^3\frac{f}{\alpha}\zeta} \cong 1 - i2p_o'^3\frac{f}{\alpha}\zeta - 4p_o'^6\frac{f^2}{\alpha^2}\zeta^2 + \ldots \tag{12}$$

In the denominator of the integrand of Eq. (11), we approximate the same factor by only the leading term, one, since when $p_o'^3 f$ becomes appreciable, the magnitude of α tends to

#79490 - $15.00 USD Received 29 Jan 2007; revised 28 Mar 2007; accepted 1 Apr 2007; published 2 May 2007

compensate by $p_o'^{-1}$ times. In the exponent of Eq. (11), we can easily retain the corrections in Eq. (12) insofar as we allow them to contribute only to linear and quadratic terms.

After performing the integration in Eq. (11), the wavefunction becomes

$$\Psi(\vec{r},t)=\left(\frac{k_C p_o'}{\sqrt{\pi}}\right)^{3/2}\frac{1}{\alpha\sqrt{\beta}}\exp\left\{-i\eta_t^- - p_o'^2\frac{\eta_x^2+\eta_y^2}{2\alpha}-p_o'^2\frac{\eta^2}{2\beta}\right\} \tag{13}$$

where

$$\eta\equiv\eta_z+ip_o'^2\frac{f_x\eta_x+f_y\eta_y}{\alpha}+C_\eta \text{ and } \beta\equiv 1+ip_o'^2\eta_t^- + p_o'^4\frac{f_x^2+f_y^2}{\alpha}+C_\beta . \tag{14}$$

The corrections

$$C_\eta\equiv p_o'^4 f\frac{\eta_x^2+\eta_y^2}{\alpha^2} \text{ and } C_\beta\equiv -\frac{4p_o'^8 f^2}{\alpha^3}\left(\eta_x^2+\eta_y^2\right)-i\frac{4p_o'^6 f}{\alpha^2}\left(f_x\eta_x+f_y\eta_y\right) \tag{15}$$

arise from the expansion terms in Eq. (12) and often are of minor consequence and can be ignored. Moreover, these corrections can give rise to spurious contributions of no physical significance at large distances away from the wave packet, where the amplitude should approach zero. This problem is avoided by applying the formula to the 'region of interest'. Alternatively, we can avoid the corrections altogether if we retreat to the more stringent requirement $p_o'^3 f \ll 1$. Note that the approximations in Eq. (9) do not imply that terms involving orders greater than $p_o'^3$ in Eq. (15) are negligible.

5. Wave-packet dynamics

We illustrate the usefulness of Eq. (13) with several examples. Figs. 1-3 show animations generated using a laptop computer. Each frame required only a fraction of a second to calculate, making it possible to view movies while calculating on the fly. The animations in each case display a 2-D cut through the wave packet in the $y=0$ plane. Nevertheless, the dynamics described by Eq. (13) are fully three-dimensional. In accordance with standard procedure for the Klein-Gordon equation [10-12], the 'probability density' is computed from

$$\rho\equiv\frac{i\hbar}{2mc^2}\left[\Psi^*(\vec{r},t)\frac{\partial\Psi(\vec{r},t)}{\partial t}-\Psi(\vec{r},t)\frac{\partial\Psi^*(\vec{r},t)}{\partial t}\right]. \tag{16}$$

In Fig. 1(a)-(c), we show the effect of wave-packet spreading in a strong linearly polarized field, characterized by $\vec{A}=\hat{x}A_o\cos(kz-\omega t)$. Eventually, spreading causes different parts of the wave packet to interact with very different phases of the applied field. This distinctively non-dipole behavior exemplifies the sophistication of Eq. (13), which is able to accurately portray a broad range of dynamics. The momentum spread in this example was set to $p_o'=0.005$, which corresponds to an initial wave packet with a spatial extent of approximately 1Å. The scaled amplitude of the vector potential $A_o'\equiv eA_o/mc$ was set to one, which for 800 nm light corresponds to an intensity of $2.1\text{x}10^{18}$ W/cm^2. The Lorentz force causes the wave packet to drift in the z-direction (to the right). The positive x-axis is directed down the page. The movies in Fig. 1(a), (b), and (c), respectively, were generated during three intervals of equal duration: 0-10 field cycles, 50-60 field cycles, and 100-110 field cycles. Note that the Lorentz drift causes the wave packet to oscillate fewer times than the number of laser periods. The movies are positioned along the z-direction respectively at 0-2λ, 10λ -12λ, and 20λ -22λ.

#79490 - $15.00 USD Received 29 Jan 2007; revised 28 Mar 2007; accepted 1 Apr 2007; published 2 May 2007

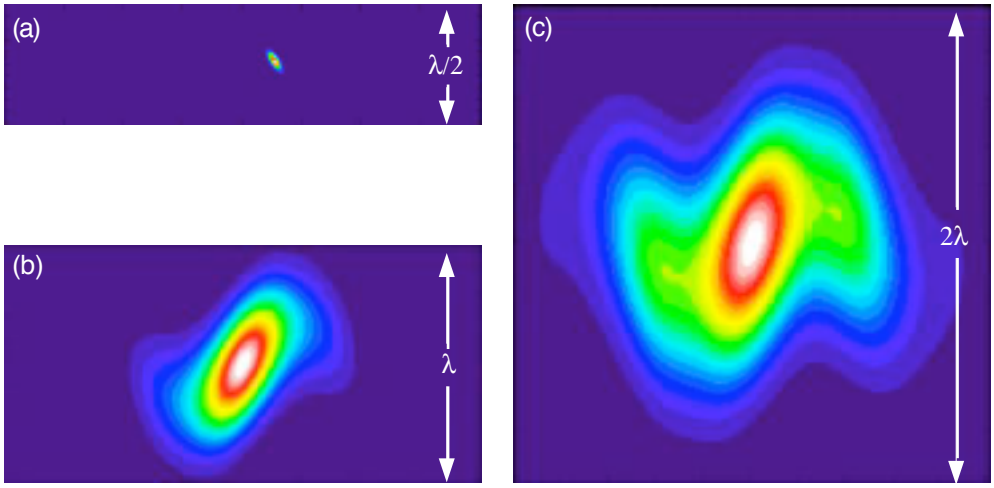

Fig. 1. (64 KB, 276 KB, 820 KB) Movies of an electron wave packet in a linearly polarized plane-wave field during (a) 0-10 cycles, (b) 50-60 cycles, and (c) 100-110 cycles. The intensity is $2.1\text{x}10^{18}$ W/cm^2 at 800 nm wavelength; the initial momentum spread is $p_o = 0.005mc$.

It is instructive to consider the conditions mandated by Eq. (9) in connection with the above example. The first and the final expressions in Eq. (9) increase without bound in time. Eventually our analytical approximation for the wave function will fail to apply. For the final frame of the movie 1(c) (t = 110 laser cycles), the expressions become $p_o'^4 k_C ct \sim 0.14$, $p_o'^3 |f_x| \sim 0.04$, and $p_o'^4 |f| \sim 0.04$, which all remain safely below one. Since the expressions are very sensitive to the momentum width p_o', a slightly narrower momentum distribution enables the approximations to hold for longer times and/or to tolerate higher applied fields.

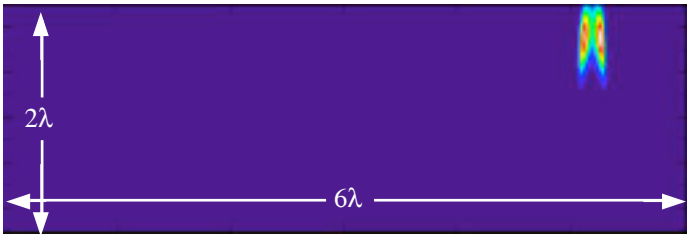

Fig. 2. (88 KB) Movie of an electron wave packet in a linearly polarized plane-wave field during 0-6 cycles. The intensity is $5.3\text{x}10^{19}$ W/cm^2 at 800 nm wavelength; the initial momentum spread is $p_o = 2\times10^{-6} mc$.

Figure 2 shows a wave packet under conditions similar to those studied by Román et al. [6]. We chose $A_o' = 5$, which corresponds to an intensity of $5.3\text{x}10^{19}$ W/cm^2. The Lorentz drift is much stronger in this example, and consequently the wave packet is significantly contracted in the z-direction. A double-hump feature, previously noted [7], is evident at each turning point. This distinctively non-dipole effect requires the wave function to have a spatial extent on scale with the laser wavelength. For this example, we created a sufficiently large wave packet by restricting the initial momentum spread via the parameter $p_o = 2\times10^{-6} mc$. This extremely small momentum range permits Eq. (13) to retain validity even at intensities many orders above that presented here. For higher intensities, the Lorentz contraction becomes more pronounced, such that the wave packet would appear as a thin vertical stripe in the movie. It is instructive to note that combining

#79490 - $15.00 USD Received 29 Jan 2007; revised 28 Mar 2007; accepted 1 Apr 2007; published 2 May 2007

the initial momentum spread of Fig. 1 with the higher intensity of Fig. 2 leads to a violation of Eq. (9) before the wave packet has time to spread to the large spatial extent seen in Fig. 2.

Figure 3 is essentially a repeat of the simulation shown in Fig. 1(b), except for circularly polarized light. In this case, the vector potential is given by $\bar{A} = \hat{x}A_o \cos(kz - \omega t) + \hat{y}A_o \sin(kz - \omega t)$. With the same value for A_o as before, the intensity doubles: 4.2x10^{18} W/cm^2. The momentum distribution was again set to $p_o' = 0.005$, the same as for Fig. 1. The movie interval for Fig. 3 ranges from 50 to 60 laser cycles, the same as for Fig. 1(b), and the frame is positioned along the z-direction from 16.5λ to 20.5λ. The continuously applied field accounts for a stronger Lorentz drift. For this movie, the peak value of the plotted probability density varies as the wave packet spirals under the influence of the circularly polarized field, moving in and out of the page. For all other animations in this article, the peak value of the wave function was normalized to one on each frame. This example explicitly demonstrates the three-dimensional character of Eq. (13).

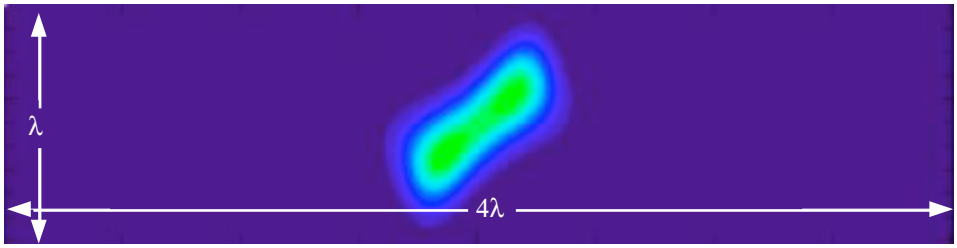

Fig. 3. (180 KB) Movie of an electron wave packet in a circularly polarized plane-wave field during 50-60 cycles. The intensity is 4.2x10^{18} W/cm^2 at 800 nm wavelength; the initial momentum spread is $p_o = 0.005mc$.

6. Dirac-Volkov solution and laser-induced spin dynamics

We wish to sketch briefly how our approach can be generalized to include the electron spin. The Volkov solution to the Dirac equation can be written as

$$\bar{\Psi}_{\bar{p},s}^{V_D}(\bar{r},t) = M \cdot \bar{u}_{\bar{p},s} \Psi_{\bar{p}}^{V_{KG}}(\bar{r},t), \tag{17}$$

where $\bar{u}_{\bar{p},s}$ is a free Dirac spinor [12], $\Psi_{\bar{p}}^{V_{KG}}$ denotes the scalar Klein-Gordon Volkov solution in Eq. (2), and

$$M - 1 = \frac{e}{2(E/c - p_z)} \begin{bmatrix} 0 & A_x - iA_y & 0 & A_x - iA_y \\ -A_x - iA_y & 0 & A_x + iA_y & 0 \\ 0 & A_x - iA_y & 0 & A_x - iA_y \\ A_x + iA_y & 0 & -A_x - iA_y & 0 \end{bmatrix}. \tag{18}$$

For definiteness, we choose

$$\bar{u}_{\bar{p},s} = \sqrt{\frac{E + mc^2}{2mc^2}} \begin{bmatrix} 1 \\ 0 \\ \dfrac{p_z c}{E + mc^2} \\ \dfrac{p_x c + ip_y c}{E + mc^2} \end{bmatrix} \tag{19}$$

to describe an electron with a positive spin component along the z axis. As before, we can construct a Gaussian wave packet from the Volkov states in Eq. (17). In the spirit of our

#79490 - $15.00 USD Received 29 Jan 2007; revised 28 Mar 2007; accepted 1 Apr 2007; published 2 May 2007

previous treatment, we employ the approximations $\vec{u}_{\vec{p},s} \cong \begin{pmatrix} 1 \\ 0 \\ 0 \\ 0 \end{pmatrix}$ and $E/c - p_z \cong mc$ in Eqs. (18) and (19). Then the superposition integral reduces to the Klein-Gordon case, aside from a momentum-independent spinor appended to the front:

$$\bar{\Psi}^D(\vec{r},t) \cong \begin{bmatrix} 1 \\ -e\dfrac{A_x + iA_y}{2mc} \\ 0 \\ e\dfrac{A_x + iA_y}{2mc} \end{bmatrix} \Psi^{KG}(\vec{r},t) . \tag{20}$$

Consequently, the standard probability density $\rho^D \equiv |\psi_1|^2 + |\psi_2|^2 + |\psi_3|^2 + |\psi_4|^2$ simplifies to

$$\rho^D \cong \left[1 + \frac{e^2\left(A_x^2 + A_y^2\right)}{2m^2c^2}\right] \left|\Psi^{KG}(\vec{r},t)\right|^2 . \tag{21}$$

Note that the prefactor in Eq. (21) can also be written as $\hbar\dot{\eta}_t^- / mc^2$. This expression is contained in the Klein-Gordon probability density Eq. (16), where it is the dominate term in the prefactor generated when performing the required time derivative. Thus, the Klein-Gordon and Dirac approaches generate essentially the same probability density.

With the help of Eq. (20), we can directly calculate the laser-driven spin dynamics of the electron. Taking into account only the spinor-valued part in Eq. (18), we find that the expectation value of the Dirac spin operators [12] are essentially given by

$$\left\langle \Sigma_x \right\rangle \cong -\frac{eA_x}{mc} , \left\langle \Sigma_y \right\rangle \cong -\frac{eA_y}{mc} , \text{ and } \left\langle \Sigma_z \right\rangle \cong 1 - \frac{e^2\left(A_x^2 + A_y^2\right)}{2m^2c^2} . \tag{22}$$

Hence, a precessive motion of the spin vector is induced [3]. We point out, however, that these are only approximations to the exact spin operators for a moving electron.

7. Conclusion

In summary, we have developed a closed analytical expression that accurately portrays a three-dimensional wave packet for a charged particle in a moderately strong electromagnetic field. The temporal envelope of the applied field is arbitrary, but it must propagate in a single direction. The initial wave packet is taken to have a Gaussian distribution in momentum. The validity of the approximation is governed by the spread of momentum in the initial wave packet, as opposed to momentum acquired during interaction with the field. The approximation breaks down eventually for large times or for large field strengths. With a narrower spread in momentum, the approximation lasts longer and tolerates higher applied fields. If the momentum distribution is chosen such that the wave packet has an initial spatial extent on the scale of an angstrom, the analytical expression remains valid into moderate relativistic conditions. How quickly the analytical solution departs from the actual one as conditions of validity are violated could be tested by comparison with corresponding numerical simulations [1,2,6,7], at the boarder of applicability of our approximation.

The approximate analytical solution presented in this article represents a useful tool, both for research and for education purposes. An array of interesting non-dipole and relativistic wave-packet dynamics can be observed and explored using very little computational overhead. The three-dimensional nature of the solution is immediately appreciated by anyone who has computed similar wave-packet dynamics numerically. To

#79490 - $15.00 USD Received 29 Jan 2007; revised 28 Mar 2007; accepted 1 Apr 2007; published 2 May 2007

our knowledge, we have presented the first animations showing the behavior of a spreading wave packet in a relativistic circularly polarized field, an intrinsically three-dimensional problem. The analysis presented here is limited to free spreading and motion of a Gaussian wave packet in a plane-wave field; it does not countenance, for example, the ionization process or collisions. A free electron wave packet obtained through tunneling/over-the-barrier ionization would likely exhibit a more complicated spatial structure. Ponderomotive gradients in a tight laser focus could also induce distortions.

We gratefully acknowledge helpful discussions with K. Z. Hatsagortsyan.

#79490 - $15.00 USD Received 29 Jan 2007; revised 28 Mar 2007; accepted 1 Apr 2007; published 2 May 2007